Field-induced structures and rheology of a magnetorheological suspension confined between two walls

2003 J. Phys.: Condens. Matter 15 S1437

(http://iopscience.iop.org/0953-8984/15/15/309)

INSTITUTE OF PHYSICS PUBLISHING JOURNAL OF PHYSICS: CONDENSED MATTER

J. Phys.: Condens. Matter **15** (2003) S1437–S1449 PII: S0953-8984(03)55038-X

Field-induced structures and rheology of a magnetorheological suspension confined between two walls

P Carletto and G Bossis

Laboratoire de Physique Matière Condensée, CNRS, Université de Nice, 06108 Nice Cedex 2, France

Received 9 October 2002
Published 7 April 2003
Online at stacks.iop.org/JPhysCM/15/S1437

Abstract

We have determined experimentally the parameters characterizing the structures formed in a magnetic colloidal suspension subjected to a unidirectional magnetic field and a rotating field for different cell thicknesses. In this latter case one observes the formation of a periodic structure in parallel sheets situated in the plane of rotation of the field. A theoretical model based on minimization of the energy allows one to find quantitatively the observations obtained in a unidirectional field. On the other hand, in a rotating field, the agreement is quantitative only if we take the surface energy as an adjustable parameter. We explain this fact on the basis of the existence of a substructure made of discs of particles. In a second part we show the influence of the structures on the rheological properties of the suspension by measuring the shear moduli for different kinds of structure. We find that for the same magnetic field, the shear moduli depend strongly on the structure and can be quite well predicted by a mean field theory; also the critical shear strain is determined and is in agreement with the model. Finally we show that, in a regime with a unidirectional oscillating field without shear flow, a new phenomenon appears if the confining walls are not parallel. In this case we observe the formation of anisotropic aggregates which undergo a collective chaotic rotation around the axis of the aggregates.

(Some figures in this article are in colour only in the electronic version)

1. Introduction

Magnetorheological (MR) suspensions are composed of magnetic particles whose size, in the micron range, is at least two orders of magnitude larger than in the better known magnetic suspensions called ferrofluids. The induced magnetostatic force between two particles scales as the square of the size of the particles and so, in the presence of an external magnetic field,

particles of micron size easily aggregate to form a gel-like structure whereas a ferrofluid remains liquid because the thermodynamic force (scaling as kT/a) is always dominant. Strong MR suspensions are made of iron particles with diameters of a few micrometres. The aggregation process for these particles is always an out-of-equilibrium process also subjected to sedimentation. In contrast, particles of diameter between 0.5 and 1 μm, made of polystyrene with magnetic inclusions of ferrous oxide, can show a phase separation with a well characterized size of the domains [1].

Such a phase separation with domain formation (usually labyrinthine structure) is well known in ferrofluids where it is possible to successfully predict the change of period of the pattern with the amplitude of the external magnetic field, if the effective surface tension at the boundary between the two phases is known [2, 3].

More recently, well defined structures formed of cylindrical aggregates aligned in the magnetic field and arranged in a hexagonal pattern have been observed in MR suspensions [4–6]. When subjected to an oscillating shear flow, these cylindrical structures transform into a striped pattern aligned in the direction of the velocity and showing a well defined period [7]. Another way to obtain a striped pattern is to apply a rotating magnetic field to the suspension because of the existence of an average attractive dipolar interaction in the plane of the rotating field [8–10].

In section 2, we first recall briefly the theory which can be used to predict the equilibrium structures resulting from a phase separation either in a constant field or in a rotating field and also in the presence of a shear flow. We shall discuss in section 3 the success and the limitation of this model on the basis of experimental results. The presence of anisotropic structures gives a lamellar composite which should present a marked anisotropy of the shear moduli. We have tested this anisotropy with a home-made plate–plate rheometer. In section 4 we present new experimental results concerning the dependence of the shear modulus on the structure and we compare with the predictions obtained from a mean field theory. Finally, we present experimental data on a new phenomenon obtained in the presence of a sinusoidal unidirectional magnetic field applied perpendicularly to a cell whose plates are not parallel to each other. We shall see that the aggregates are no longer symmetric and that they can rotate in a chaotic way around the direction of the field.

2. The model

We have to calculate the magnetic energy as a function of the structure parameters characterizing the domains. In the case of a unidirectional field the domains usually have a symmetry of revolution around the field and, for the sake of simplicity, we consider that they have an ellipsoidal shape and that they are located on a hexagonal array. For the case of a rotating field—or for a constant field and a shear flow—we observe a striped structure and we characterize the domains by layers of particles which are equally spaced from each other. The minimum distance, d, between the domains and their size (or their internal volume fraction: Φ_a) are the two parameters that we are looking for. We suppose that between the domains there are no particles (the osmotic pressure of the colloidal particles is zero). The two parameters are then obtained through a minimization of the magnetic energy, U_m, and an equilibrium of the magnetic pressure, P_m, and of the osmotic pressure, P_{osm} inside the domains:

$$\frac{\partial}{\partial d}(U_m/V)_\varphi = 0 \qquad \text{and} \qquad P_m + P_{osm} = 0.$$

2.1. Magnetic energy of a hexagonal array of ellipsoids

Let us consider a two-dimensional hexagonal array of N_a ellipsoidal aggregates of semi-axis b and length $h = 2l$ and separated by a distance d. The following notation is used: M_a is the magnetic moment of one aggregate and V_a its volume. The quantity $\varphi = N_a V_a / V$ is the part of the volume which is occupied by the aggregates. It must not be confused with the internal volume fraction inside the aggregate $\Phi_a = \Phi_0/\varphi$ where Φ_0 is the average volume fraction of particles in the suspension. The magnetic moment M_a of an ellipsoidal aggregate is given by [6]

$$M_a = \frac{\mu_a - 1}{4\pi}\left[\frac{H_0 - \sum_j T_{ij}^r M_a}{1 + n_z(\mu_a - 1)}\right]V_a = \alpha_a\left(H_0 - \sum_j T_{ij}^r M_a\right) \tag{1}$$

where $\mu_a = f(\Phi_a)$ is the permeability of the aggregate obtained by using the equation of Maxwell-Garnett; n_z is the demagnetization factor of an ellipsoid:

$$n_z = \frac{(1-e^2)}{2e^3}\left(\ln\left(\frac{1+e}{1-e}\right) - 2e\right) \qquad \text{with } e \text{ the eccentricity: } e = (1 - b^2/l^2)^{1/2}.$$

$T_{ij}^r = (1/h^2)[2/d_{ij} - 2/(d_{ij}^2 + h^2)^{1/2}]$ is the propagator of the field due to aggregate j on the aggregate i whose axes are separated by the distance d_{ij} [4]. The total magnetic energy per unit volume is then

$$\frac{U_m}{V} = \frac{-1}{2V} N_a \vec{M}_a \cdot \vec{H}_0 = \frac{-\varphi H_0^2}{8\pi}\left[\frac{(\mu_a - 1)}{1 + n_z(\mu_a - 1)}\right]\left[\frac{1}{1 + n_r}\right] \tag{2}$$

with

$$n_r = \sum_j T_{ij}^r = \left[\frac{(\mu_a - 1)}{1 + n_z(\mu_a - 1)}\right][\varphi]\left[\sqrt{\left(1 + \frac{d^2}{h^2}\right)} - \frac{d}{h}\right] \qquad \text{and} \qquad d = b\sqrt{\frac{2}{3\varphi}}.$$

Finally, we have also to take into account the surface tension of the aggregate, σ, coming from the change of local field on the particles belonging to the surface S_a of an aggregate. Indeed, the magnetic field is weaker on the surface than inside the aggregate and the corresponding energy is [7]

$$\frac{U_S}{V} = \frac{N_a \sigma S_a}{V} \qquad \text{with } \sigma = \frac{M_a^2 a}{3\mu_0 V_a^2}. \tag{3}$$

This term must be added to the right-hand side of equation (2). In the following derivation we shall show how it can be included in the magnetic energy from the beginning.

2.2. Magnetic energy of a layered structure

The average interaction in the plane of rotation of the field is attractive and induces the formation of a layered pattern. We call the thickness of the layer e and its height h. We suppose that the width L is very large compared to the other dimensions, so we consider a two-dimensional situation. Let us write $\vec{H}_0^n$ for the component of the field normal to the plane of the cell and $\vec{H}_0^t$ for the tangential component: $\vec{H}_0 = \vec{H}_0^n + \vec{H}_0^t$. These two components are sinusoidal with a phase difference of $\pi/2$. The particles that we use are superparamagnetic and the magnetization does not show any hysteresis at the frequencies used ($\nu < 50$ Hz), so we can treat each component independently. Due to this simple geometry we can reason at the level of one particle and write for the normal magnetic moment of a layer $M_a^n = N_V m_V^n + N_S m_S^n$ with $N_v m_V^n$ and $N_s m_S^n$ respectively the number of particles and the magnetic moment of a given

particle in the volume of the aggregate and on its surface. The magnetic energy U_{layer} of a layer of paramagnetic particles in a rotating field is then

$$U_{layer} = -\tfrac{1}{4}[M_a^n H_0^n + M_a^t H_0^t]. \tag{4}$$

The magnetic moment of a particle inside the aggregate will be the product of its polarizability, α, and the local field, H_{loc}:

$$m_V^n = \alpha H_{loc} = \alpha\left(H_0^n - 4\pi n_d \frac{M_a^n}{V_a} + \frac{4\pi}{3}\frac{M_a^n}{V_a}\right) \qquad \text{with } \alpha = a^3\frac{(\mu_p - 1)}{(\mu_p + 2)} = \beta a^3. \tag{5}$$

The second term in the right-hand side of (5) is the demagnetization field and the third one is the Lorentz field inside the layer. For a particle on the surface, we divide the Lorentz field by two, so we have

$$m_S^n = m_V^n - \frac{2\pi}{3}\alpha\frac{M_a^n}{V_a}. \tag{6}$$

Using equations (5), (6), we obtain the normal component of the magnetic moment of a layer per unit volume:

$$M_n = \frac{M_a^n}{V_a} = \frac{3\beta\Phi_a/4\pi}{1 - \beta\Phi_a(1 - 3n_d - 2a/e)}H_0^n. \tag{7}$$

For the tangential component of the magnetic field, the method will be the same but with a significant simplification, since in this case the demagnetizing factor is zero. We thus have the result given by equation (7) but with $n_d = 0$ and H_0^t instead of H_0^n. Using equations (4)–(7), we can calculate the total energy per unit of volume. In our case, $H_0^t = H_0^n$ (rotating field) and we obtain

$$\frac{U_m}{V} = \frac{3\beta H_0^{n^2}\Phi_0 A}{16\pi} \qquad \text{with } A = \frac{1}{1 - \beta\Phi_a(1 - 3n_d - 2a/e)} + \frac{1}{1 - \beta\Phi_a(1 - 2a/e)}. \tag{8}$$

The value of the demagnetizing factor n_d for a layered pattern with a period d was already calculated by Cebers [11]:

$$n_d(\varphi, d) = \varphi + \frac{d}{\pi^3\varphi}\sum_{k=1}^{+\infty}\frac{\sin^2(\pi k\varphi\varphi)}{k^3}\left(1 - \exp\frac{-2\pi k}{d^*}\right) \qquad \text{with } d^* = \frac{d}{h}. \tag{9}$$

Note that in equation (8) the surface energy does not appear explicitly, but through the term a/e.

2.3. Balance of pressures

Assuming that the total pressure (magnetic pressure plus osmotic pressure) inside the aggregates is close to zero for well formed domains, we get an other equation allowing us to determine the second unknown which is the internal fraction, Φ_a, inside the aggregates. The magnetic and osmotic pressures are respectively

$$P_m = \frac{\partial}{\partial V}(U_m)\bigg|_d \qquad \text{and} \qquad P_{osm} = \frac{kT}{v_p} \times 1.85 \times \frac{\Phi_a}{0.64\Phi_a} \tag{10}$$

(v_p is the volume of the particle). The last expression for the osmotic pressure comes from molecular dynamics or Monte Carlo simulations of hard spheres [12]. This is clearly an approximation since the structure inside the domains is anisotropic due to the presence of the magnetic field and numerical simulations should help us to find a better approximation.

Another point which is worth stressing is the contribution of a shear flow to the osmotic pressure. A shear flow with the velocity and the velocity gradients defining the plane of the

layered structure will increase the diffusivity of the particles in the direction perpendicular to the layers, which can be expressed by a shear-induced osmotic pressure. A simple hypothesis is to consider that this pressure is proportional to the fluctuations of velocity which scale as the square of the shear rate and that it will diverge close to the maximum packing fraction of 0.64 in order to be coherent with equation (10). Such an implementation was shown to be quite successful in reproducing the experimental results for the period of a layered structure obtained in the presence of a shear flow and of a constant magnetic field [7].

3. Experimental determination of the field-induced structures

The suspension is placed between two glass plates making a small angle with each other in order to produce a variable thickness from one extremity of the cell to the other. This cell is sealed and can be filled with a syringe. It is placed at the centre of Helmholtz coils and we observe the structure with the help of a microscope equipped with a video camera. The magnetic field is driven by a computer which also records the pictures of the structure. The suspension that we have used is made of polystyrene particles containing 63% by weight of magnetite. These particles, designed by Merck, suspended in water are spherical but slightly polydisperse, with an average diameter of 0.78 μm for all experiments presented in this paper. They behave as a superparamagnetic material and their initial permeability was obtained from a measurement of the flux variation in a coil containing the suspension in the presence of a sinusoidal current. We find $\mu_p = 2.69$ for both samples. The corresponding magnetic moment of the particle placed in the external field H_0 is

$$m_p = 4\pi a^3 \mu_0 \beta H_0 \qquad \text{with } \beta = (\mu_p - 1)/(\mu_p + 2).$$

The main quantity which will control the phase separation in the absence of shear is the ratio of the magnetic dipolar energy to the thermal energy:

$$\lambda = \frac{2m_p^2}{4\pi\mu_0(2a)^3 kT} = \frac{\pi\mu_0\beta^2 a^3 H_0^2}{kT}$$

which gives for $a = 0.39$ μm, $\beta = 0.36$ and room temperature: $\lambda = 6.83 \times 10^{-6} H_0^2$ with H_0 in A m^{-1} or, since $B_0 = \mu_0 H_0$, $\lambda = 8.66 \times 10^6 B_0^2$ with B_0 in teslas. We see that even for fields as low as 3.4×10^{-4} T (or 3.4 G) the magnetic force already dominates the thermal forces.

3.1. Experimental results

The cell is placed at the centre of two pairs of Helmholtz coils which are located in such a way that the plane of rotation of the field is perpendicular to the plane of the cell. The two coils are supplied with two voltages presenting a phase difference of $\pi/2$. A schematic view of the geometry of the rotating field with respect to the cell is represented in figure 1(a).

This device can also be used to study the structure in the case of a unidirectional field (here along Ox) by supplying only one pair of coils with a DC. The results obtained with a unidirectional field for different cell heights have been reported elsewhere [10]. We have found that for an initial volume fraction $\Phi_0 = 0.045$ we can fit the experimental data very well with a power law: $d = 0.8h^{0.5}$, with d the average distance between aggregates and h the thickness of the cell which was between 40 and 1000 μm. The value of the field was $H = 76$ Oe (corresponding to $\lambda = 268$). The theoretical model predicts $d = 0.95h^{0.49}$ for this given range of thickness. Since there are no adjustable parameters, this prediction is in fair agreement with the experiment. It should also be understood that these power laws are only a convenient way to reproduce the results for a limited range of thicknesses: there is no

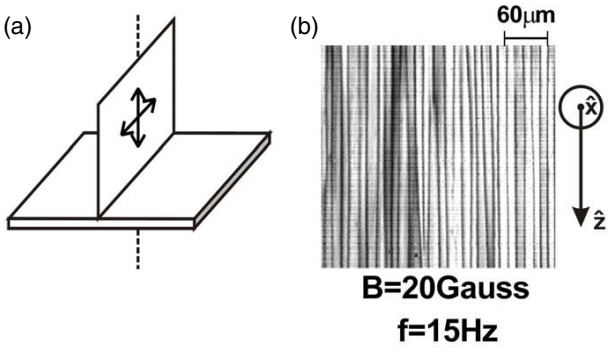

Figure 1. The geometry of the experiment. (a) The suspension is placed between the two plates; the broken line is the axis (Ox) of observation. (b) The top view of the cell. The field is rotating in the plane Oxz as indicated by the arrows in (a).

simple analytic law for the variation of the distance between the aggregates versus the sample thickness.

Let us now discuss in some more detail what happens in a rotating magnetic field. The image that we can see in this case is reproduced in figure 1(b). We have a phase separation with the formation of thin layers of particles. The thickness of one layer is a few micrometres, which represents a few particle diameters.

When the frequency of rotation of the field is high enough that a pair of particles do not move appreciably during one period, then we have an average attractive interaction which is responsible for the formation of discs of particles in the plane of rotation of the field. In fact, the average energy of two dipoles rotating in phase with the field is $U = (-m^2/2r^3)(1-3\cos^2\theta)$, where θ is the angle between the normal to the plane of the rotating field and the vector $\vec{r}$ joining the two dipoles. This interaction is attractive for $\theta = \pi/2$ (dipoles in the plane of rotation) and repulsive for $\theta = 0$; so it induces a layered pattern with the normal to the layers parallel to the axis of rotation of the magnetic field [8].

Due to the symmetry of the rotating field, we expect the particles to first gather in disc-shaped aggregates, which will join each other at higher field to form a layered structure. It is then tempting to use a cylindrical cell—that is to say, a capillary—in order to see how the shape of the container can influence the period of the structure. The model described in section 2 must be slightly modified: firstly we have only to consider the normal field component and secondly the demagnetization factor, n_d, in equation (9) will be different.

The calculation shows that the period of the layered structure in a capillary of diameter $2h$ should be the same as that of a thin cell of thickness h. The geometry is shown in figure 2(a) and the experimental period, in both situations, is plotted in figure 2(b) versus the frequency of the rotating field for two different fields: 15 and 20 G. We see that the difference in period between the two geometries is indeed quite small and practically within the uncertainty bars. Furthermore, it appears that in this frequency domain the period of the layered structure is independent of the rotation frequency, as we could expect for high enough frequencies. We also observe in figure 2(b) that between 15 and 20 G the period has decreased from 10 to 8 μm. For higher fields the period will no longer change. In fact, the structure begins to appear for 9 G with a period of about 11 μm. The decrease of period with the increase of the field could probably be predicted if we were able to introduce in the model a structure with two different volume fractions Φ_1 and Φ_2 instead of Φ_a and 0. The comparison with the model has been realized in the high-field domain, where it applies, and the results are plotted in figure 3.

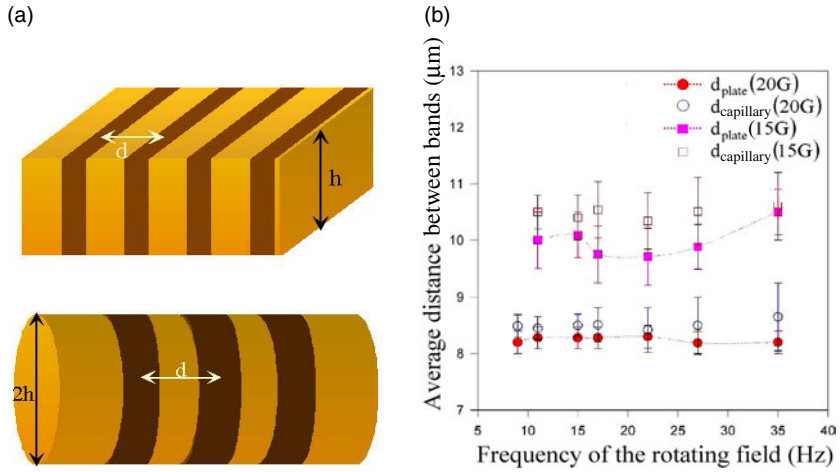

Figure 2. (a) Domains in a rotating field with two different geometries (flat cell and capillary); the plane of rotation of the field is perpendicular to the axis of the capillary. (b) Average distance between layers versus frequency of the rotating field. The solid symbols correspond to the flat cell and the open ones to the capillary. Upper curves: $H = 20$ G; lower ones: $H = 15$ G.

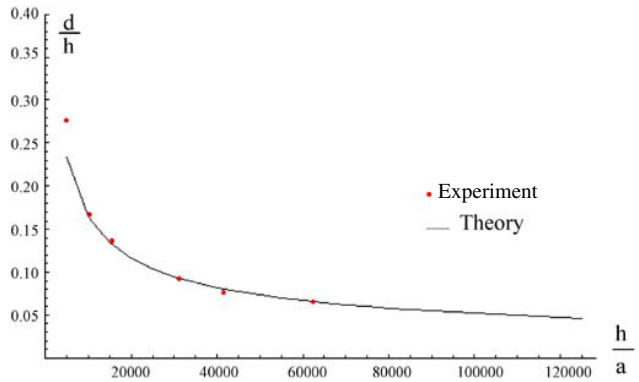

Figure 3. The change of average inter-aggregate distance normalized by the height of the cell h, versus the thickness of the cell, h, normalized by the radius of the particles a.

The agreement is quite good but we have to note that we took the surface tension as a parameter. The surface tension comes from the change of the Lorentz field on the boundary of the domain whose thickness is proportional to the radius of a particle (the term a/e of equation (8)). In order to obtain a good fit we were obliged to decrease the surface tension by almost two orders of magnitude. An explanation of this discrepancy could be that, in practice, the layers observed in a rotating magnetic field are not homogeneous but present a substructure made of disc-shaped aggregates having a thickness of one particle and also a radius probably smaller than the thickness of the cell. Some support for this explanation comes from the observation of the structure when the field is rotating in the plane of the cell. We see in figure 4 that the structure is not homogeneous at all and presents many holes. Also, numerical simulations show that the stripes of particles are composed of several monolayers of particles [13].

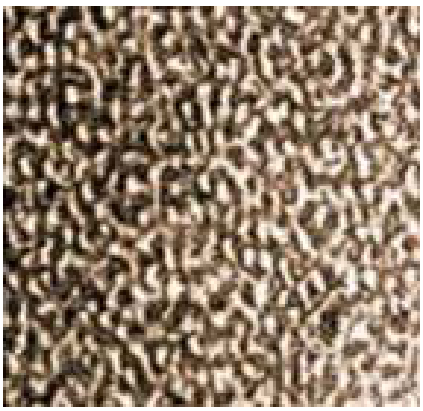

Figure 4. A top view of the plane of particles. The field, of amplitude 20 Oe, is rotating in the plane of the figure. The thickness of the suspension is $h = 50$ μm.

4. Anisotropy in the elastic shear modulus of the layered structures

The application of a rotating field to a magnetic suspension allows one to create a mesoscopic structure made of parallel layers spaced by an average distance d. Such sheets of particles also form in steady shear flow in the presence of a constant field, where they are aligned in the plane formed by the velocity and the field. The presence of these structures has a large influence on the rheology of the magnetic suspension, but if they are formed by the flow the interplay between the structure and the rheology is quite complex. Here we have the opportunity to form such layers in the absence of a flow and then to measure their rheological properties by applying a small shear rate in order to keep them intact. We have done this experiment using a home-made plate–plate rheometer. The suspension is placed between two glass discs; the upper one is fixed on the arm of an electromagnetic vibrator and the lower one on a vertical stage with submicron resolution of the displacement. The adjustment of the parallelism is carried out by looking at the Fabry–Perot fringes produced by the reflections of a laser beam between the two plates. The horizontality of the cell is also adjusted with the help of the reflections of the laser beam by the glass discs. The error in the parallelism is less than 1 μm over the whole surface and the error in the average thickness of the cell is less than 2 μm.

After the liquid has been introduced with a syringe, the lower plate is raised to a fixed distance from the upper one ($<$500 μm because the liquid is held by capillary forces). The horizontal displacement of the upper plate is measured with an optical detector which detects the change of the light reflected by a small mirror mounted on the upper plate. The magnetic field is driven by a computer which also records the upper plate displacement and the voltage applied to the electromagnet transducer; this voltage is proportional to the shear force applied to the suspension. The ratio of the amplitude of the force to the amplitude of the displacement, together with the phase difference, allows us to measure the viscoelastic properties of the suspension, namely $G'(\omega)$ and $G''(\omega)$. In practice, the dissipation of the membrane holding the vibrating rod is too large, compared to the viscous friction of the liquid, and only $G'(\omega)$ can be determined with a good sensitivity. We were also able to check the displacement signal with an oscilloscope. In fact, when the signal is no longer sinusoidal, we have seen with a microscope that it corresponds to the point where the aggregates begin to break. We shall come back to this point later.

We first measured the value of G' versus frequency for the columnar structure obtained in a unidirectional field. We find $G' = 17$, 27.5 and 36 Pa for respectively $H = 190$, 230

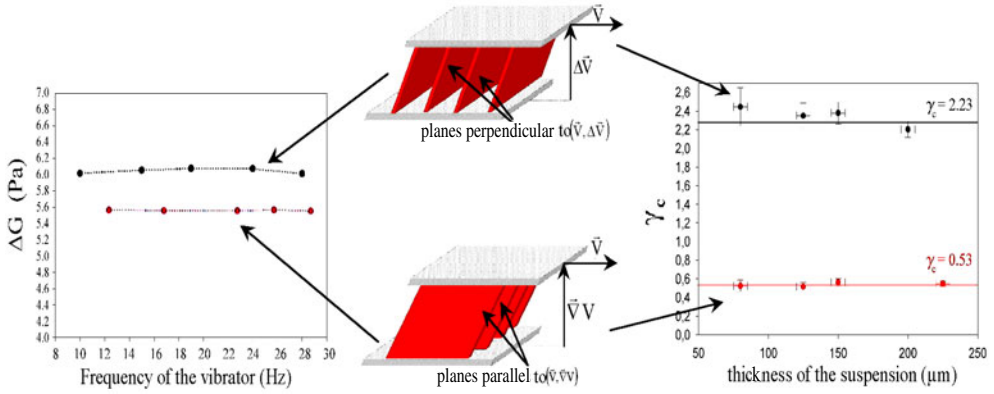

Figure 5. Left: variation of the elastic modulus versus the frequency of rotation of the field. Upper curve: layers perpendicular to the strain; lower curve: parallel to the strain. The amplitude of the field is 20 Oe, the frequency of rotation is 18 Hz and $\gamma = 0.1$.

and 270 Oe. The dependence on frequency in our range of measurement (25–36 Hz) was not significant. The measurements were made for a small strain: $\gamma = 0.1$, which does not modify the columnar structure. Increasing the strain until $\gamma = 0.3$, the structure changed to form a layered structure in the plane of the velocity and field. Now, coming back to $\gamma = 0.1$, we no longer measure the same shear modulus but a higher one: $G' = 26.5$, 38 and 59 Pa for the same fields. This means that the stripe structure is more difficult to strain in the presence of a field that the individual columns. Now we can also build a layered structure perpendicular to the lines of flow by using the mean rotating field. Due to the coils used to produce the rotating field, its value is much lower than for a constant one; so we have to compare the value of G' for two layered geometries obtained with the same rotating field (cf the left-hand part of figure 5). The result is that the shear modulus of the layers strained in their own plane ($G' = 6$ Pa) is slightly higher than if they are strained in a perpendicular direction ($G' = 5.6$ Pa). In both cases the amplitude of the rotating field was $H = 16$ Oe. On the right in figure 5 we have plotted the critical strain corresponding to the rupture of the aggregates. For the perpendicular situation the critical strain, $\gamma_c = 0.53 \mp 0.07$, is much lower than for the parallel case: $\gamma_c = 2.3 \mp 0.27$.

It is possible to compare these results with some theoretical predictions based on a mean field theory: the aggregates (either planes or cylinders) are considered as a continuous medium of volume fraction Φ_a. The change of energy of these aggregates, when they are strained in a constant magnetic field, can be calculated by considering the change of magnetic energy, W, of a composite medium [14, 15]. The shear stress will be given by the derivative of the energy relative to the strain:

$$\tau = \frac{F_y}{S} = -\frac{1}{S}\frac{\partial W}{\partial y} = -\frac{1}{V}\frac{\partial W}{\partial \gamma} = \frac{1}{2V}H_0\frac{\partial m_z}{\partial \gamma} \qquad \text{with } W = -\frac{1}{2}\vec{m}\cdot\vec{H}_0 \text{ and } \gamma = \frac{y}{h}$$

where m_z is the component of the magnetic moment of the sample in the direction of the magnetic field.

Following these lines, we obtain for the shear stress the following expression [15]:

$$\frac{\tau}{\mu_f H^2} = -\frac{1}{2}(\mu_a^*)^2\frac{2\gamma}{(1+\gamma^2)^2}\frac{\varphi(1-\varphi)}{C_s + \mu_a^*(1-\varphi)} \qquad \text{with } \varphi = \frac{\Phi_0}{\Phi_a} \text{ and } \mu_a^* = \frac{\mu_a}{\mu_f} - 1. \quad (11)$$

$C_s = 1$ for a planar aggregate and $C_s = 2$ for cylinders. The quantity μ_f is the permeability of the suspending fluid.

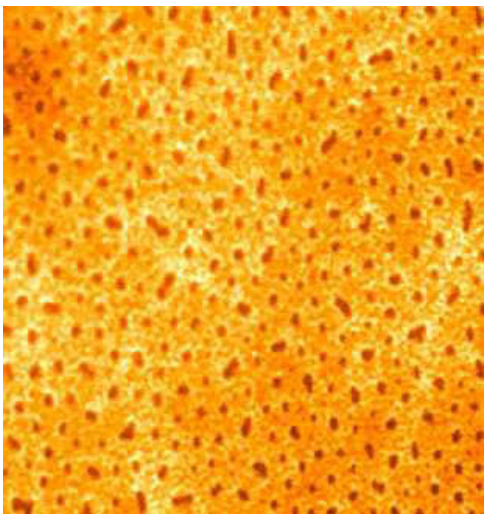

Figure 6. A top view of the aggregates. The sinusoidal field is perpendicular to the plane of the figure. The frequency and the amplitude of the field are 15 Hz and 60 Oe. The local height is 800 μm and the angle is 1.48°.

The slope for small values of γ is the shear modulus. In order to evaluate G' we need to know the volume fraction Φ_a inside the aggregates. We could use the equations given in section 2, but we know that when $\lambda \gg 1$ we are close to a compact volume fraction that we can take equal to 0.64. This is the case for $H = 200$ Oe (but not in the case of the rotating field with $H = 16$ Oe which is close to the critical field of 8 Oe). The volume fraction in this experiment was $\Phi_0 = 0.1$. The permeability of the particles was $\mu_p = 2.69$. From the measurement of the magnetization and the application of the Maxwell-Garnett formula we obtain $\mu_a^* = 0.88$. The value of the shear modulus from equation (11) is then $G' = 15.4$ Pa for $H = 230$ Oe rather than 27.5 for the experimental value. For stripes perpendicular to the strain direction, equation (11) predicts $G' = 24.3$ Pa, which we can compare with the experimental result: $G' = 38$ Pa, but with stripes parallel to the strain. This is an upper bound, since we have seen that the perpendicular case gives a lower modulus. In any event it appears that equation (11) gives the right order of magnitude and a good trend when we change from cylinders to stripes.

Another piece of information that can be obtained from equation (11) is the critical shear rate where we expect the aggregates to break. In fact, this will happen for the strain corresponding to the maximum of the stress–strain curve. This maximum is found to be $\gamma_c = \frac{1}{\sqrt{3}} = 0.57$. This theoretical value is in good agreement with the experimental value of 0.53.

When the layers are strained in their own plane, the model does not apply, but we can clearly expect a significant effect of breaking and recombination of the chains inside the layers well before the critical strain of 2.23.

5. Structures in a unidirectional sinusoidal field and with non-parallel walls

We were using a cell with non-parallel walls in order to facilitate the measurements of the structures for different heights of the cell. We were quite surprised to see that, when subjected to a sinusoidal field perpendicular to the lower wall of the cell, the aggregates first lose their cylindrical symmetry and secondly begin to rotate around the axis of the field in a chaotic way.

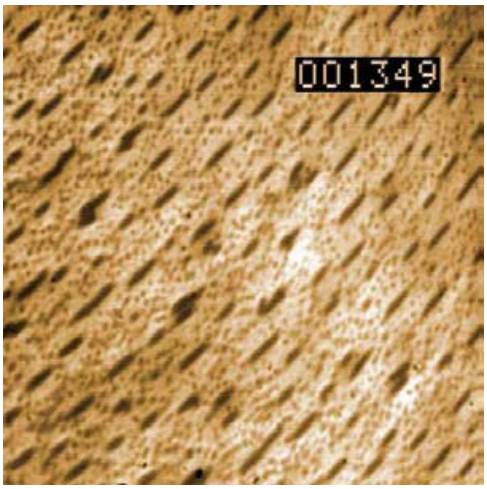

Figure 7. A top view of the aggregates. They make an angle of 45° with the direction of the gradient of the height. The conditions are the same as for figure 7 except the frequency, which is 35 Hz.

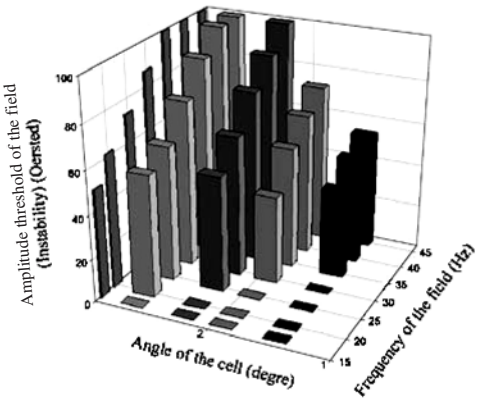

Figure 8. Change of the field amplitude threshold for which the instability appears versus angle of inclination of the cell and frequency of the field.

For instance, we can see in figure 6 that the aggregates still have a cylindrical symmetry for a frequency of 15 Hz but that this is no longer the case for a frequency of 35 Hz. In this last case the orientation of the aggregates oscillates in a chaotic way among three directions, one along the gradient of height of the cell, another at about 45° as shown in figure 7 and the third one at 135°.

It appears that increasing the angle between the two walls increases the threshold frequency above which the phenomenon happens but reduces the threshold amplitude of the field, as can be seen in figure 8. It is also important to note that this chaotic motion does not take place throughout the whole cell but in a reduced part of it. When the amplitude of the field is increased, the location of the instability drifts towards larger heights, as can be seen in figure 9. Another interesting feature of this instability is that all the aggregates have the same chaotic motion in the part of the cell where this motion takes place.

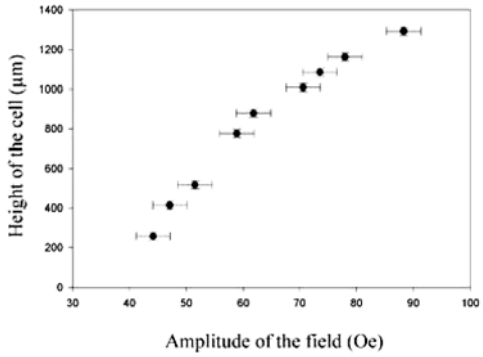

Figure 9. Location in the cell of the instability versus amplitude of the field. The angle of the cell is 1.48° and the frequency of the field is 35 Hz.

We can try to interpret this motion by saying that due to the angle, and to the magnetization of the aggregates, there is a tangential component of the field. This component can explain the loss of the cylindrical symmetry. Furthermore, we need a relaxation process in order to be able to generate a torque on the aggregate. This relaxation process can come from the Brownian motion of the particles inside the aggregate or, perhaps, from the relaxation time of the magnetization inside the particles. The use of particles of different sizes should help us to understand the origin of this relaxation time. Also, experiments with a larger cell would allow us to make more precise measurements of the location of the instability and the effect of the boundaries of the cell.

6. Conclusions

In this paper, we have shown that magnetic suspensions made of colloidal particles of size slightly smaller than 1 μm constitute a good material with which to test the theories of phase separation and domain formation in the presence of a magnetic field. Such a size allows a direct observation of the structures with a microscope and the magnetic forces between particles are large enough to give significant rheological effects; yet still the Brownian motion is high enough for avoiding out-of-equilibrium aggregation. The shape of the domains depends on the geometry of the cell. A model of minimization of the free energy well reproduces this dependence but should include, for a more exact theory, the state of the internal structure inside the domains. We have measured, in the presence of layered domains, a shear modulus that depends on the strain direction. Mean field theories applied to the calculation of the deformation of magnetic domains in a constant field reproduce the experimental behaviour quite well.

We have shown that not only does the separation between the two confining walls determine the average separation and thickness of the domains, but also the presence of a small angle between these walls can completely change the structure and generate a local motion inside the cell in the presence of a sinusoidal perpendicular field.

Acknowledgment

We are grateful to A Cebers for many helpful discussions.

References

[1] Bossis G, Volkova O, Lacis S and Meunier A 2002 *Magnetically Controllable Fluids and Their Application (Springer Lecture Notes in Physics vol 594)* ed S Odenbach (New York: Springer) pp 186–218
[2] Cebers A 1990 *Magnetohydrodynamics* **26** 309
[3] Buyewitch Yu A and Zubarev Yu A 1993 *J. Physique* II **3** 1633
[4] Lemaire E, Bossis G and Grasselli Y 1993 *J. Physique* II **2** 359
[5] Liu J *et al* 1995 *Phys. Rev.* E **74** 2828
[6] Grasselli Y, Bossis G and Lemaire E 1994 *J. Physique* II **4** 253
[7] Cutillas S, Bossis G and Cebers A 1998 *Phys. Rev.* E **57** 804
[8] Halsey T C, Anderson R A and Martin J E 1995 *Proc. 5th Int. Conf. on Electrorheological Fluids, Magnetorheological Suspensions and Associated Technology* ed B Bullough (Singapore: World Scientific) p 192
[9] Bossis G, Carletto P, Cutillas S and Volkova O 1999 *Magnetohydrodynamics* **35** 371
[10] Carletto P, Bossis G and Cebers A 2002 *Int. J. Mod. Phys.* B **16** 2279
[11] Cebers A 1995 *J. Magn. Magn. Mater.* **149** 93
[12] Russel W B, Saville D A and Schowalter W R 1989 *Colloidal Dispersions* (Cambridge: Cambridge University Press)
[13] Men S, Meunier A, Métayer C and Bossis G 2002 *Int. J. Mod. Phys.* **16** 2363
[14] Rosensweig R E 1995 *J. Rheol.* **39** 179
[15] Bossis G, Lemaire E, Volkova O and Clercx H 1997 *J. Rheol.* **41** 687